

Extending cross metathesis to identify selective HDAC inhibitors: synthesis, biological activities and modelling

Samuel Bouchet, Camille Linot, Dusan Ruzic, Danica D. Agbaba, Benoit Fouchaq, Joëlle Roche, Katarina Nikolic, Christophe Blanquart, and Philippe Bertrand

ACS Med. Chem. Lett., **Just Accepted Manuscript** • DOI: 10.1021/acsmchemlett.8b00440 • Publication Date (Web): 09 May 2019

Downloaded from <http://pubs.acs.org> on May 9, 2019

Just Accepted

“Just Accepted” manuscripts have been peer-reviewed and accepted for publication. They are posted online prior to technical editing, formatting for publication and author proofing. The American Chemical Society provides “Just Accepted” as a service to the research community to expedite the dissemination of scientific material as soon as possible after acceptance. “Just Accepted” manuscripts appear in full in PDF format accompanied by an HTML abstract. “Just Accepted” manuscripts have been fully peer reviewed, but should not be considered the official version of record. They are citable by the Digital Object Identifier (DOI®). “Just Accepted” is an optional service offered to authors. Therefore, the “Just Accepted” Web site may not include all articles that will be published in the journal. After a manuscript is technically edited and formatted, it will be removed from the “Just Accepted” Web site and published as an ASAP article. Note that technical editing may introduce minor changes to the manuscript text and/or graphics which could affect content, and all legal disclaimers and ethical guidelines that apply to the journal pertain. ACS cannot be held responsible for errors or consequences arising from the use of information contained in these “Just Accepted” manuscripts.



Extending cross metathesis to identify selective HDAC inhibitors: synthesis, biological activities and modelling.

Samuel Bouchet¹, Camille Linot², Dusan Ruzic³, Danica Agbaba³, Benoit Foucaq^{4,5}, Joëlle Roche^{5,6}, Katarina Nikolic³, Christophe Blanquart^{2,5}, Philippe Bertrand^{1,5*}.

1 Institut de Chimie des Milieux et Matériaux de Poitiers, UMR CNRS 7285, 4 rue Michel Brunet, TSA 51106, B28, 86073, Poitiers cedex 09, France.

2 CRCINA, INSERM, Université d'Angers, Université de Nantes, Nantes, France.

3 Department of Pharmaceutical Chemistry, Faculty of Pharmacy, University of Belgrade, Vojvode Stepe 450, 11000 Belgrade, Serbia.

4 Eurofins-Cerep, Le Bois l'Evêque, 86600 Celle – L'Evescault, France.

5 Réseau Epigénétique du Cancéropôle Grand Ouest. France.

6 Laboratoire EBI, University of Poitiers, UMR CNRS 7267, F-86073 Poitiers, France.

KEYWORDS: *Cross metathesis, Histone deacetylases, lung cancer, epigenetics, molecular modeling.*

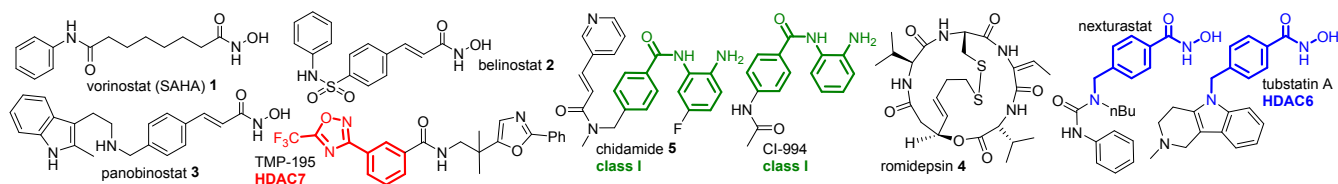
ABSTRACT: Dissymmetric cross metathesis of alkenes as a convergent and general synthetic strategy allowed for the preparation of a new small series of HDAC inhibitors. Alkenes bearing BOC-protected hydroxamic acid and benzamide and trityl-protected thiols were used to provide the zinc binding groups and were reacted with alkenes bearing aromatic cap groups. One compound was identified as a selective HDAC6 inhibitor lead. Additional biological evaluation in cancer cell lines demonstrated its ability to stimulate the expression of the epithelial marker E-cadherin, and tumor suppressor genes like SEMA3F and p21, suggesting a potential use of this compound for lung cancer treatment. Molecular docking on all eleven HDAC isoforms was used to rationalize the observed biological results.

Human histone deacetylases (HDAC) and their inhibitors (HDACi) are part of the therapies used to treat human cancers, with four HDACi approved by FDA: SAHA **1**¹ (suberoyl anilide hydroxamic acid, Chart 1, vorinostat) for cutaneous T-cell lymphomas (CTCL), belinostat **2**² for relapsed or refractory peripheral T-cell lymphoma (PTCL), panobinostat **3** for multiple myeloma,³ and FK228 **4**⁴ (romidepsin) for CTCL. Chidamide **5** (Tucidinostat) is approved only in China for PTCL.⁵ Nevertheless, solid tumour treatments with epigenetic compounds is still needed.⁶ HDACs participate in the regulation of gene expression by epigenetic mechanisms affecting chromatin structure and function.⁷ HDACs are a subgroup of eleven zinc-dependent proteins that deacetylate lysine residues of proteins including the core nucleosomal histones H3, H4, H2A and H2B, leading in turn to the repression of gene expression. Some HDAC deacetylate non-histone proteins, like HDAC6 for tubulin. HDACs are grouped in three classes, class I (HDAC1-3, 8), class II (IIa HDAC4, 5, 7, 9 and IIb HDAC6,10) and class IV (HDAC11). The seven NAD-dependent sirtuins (SIRT1-7) represent the class III

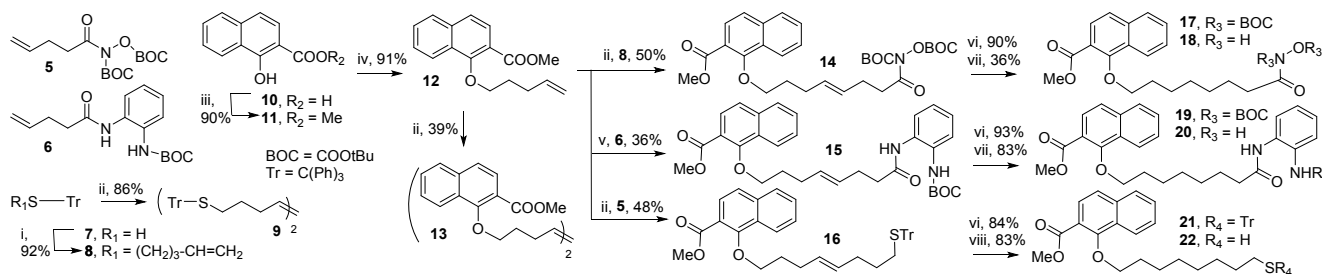
Chart 1. Some HDAC inhibitors illustrate cap/ZBGs selectivity profiles.

deacetylases. The over-expression of HDACs in cancer cell lines is correlated with the repressed expression of tumour suppressor genes (TSG),^{8,9,10} and HDACi are evaluated alone or in combination.¹¹

HDACi are composed of a zinc-binding group (ZBG) linked by a carbon structure to a “cap” group, mostly aromatic,¹² in interaction with the HDACs external solvent accessible surface. HDACi limitations' are their pharmacokinetics, the side effects at the effective dosing and resistance,¹³ possibly avoided by systemic low dosing administration for a better renormalization of cancer cells.⁶ Bulk substituents and the absence of amide bonds may favour the plasma stability of hydroxamates¹⁴ in various species. The lack of selectivity of clinically approved HDACi limits their specific applications.¹⁵ The selectivity against class I HDACs results from para-substituted benzamide inhibitors,¹⁶ 4-alkylaminomethylbenzhydroxamic acid scaffold, as in tubastatin or nexturastat, gives HDAC6 selectivity,¹⁷ whereas the trifluoromethyloxadiazole TMP-195 has HDAC7 selectivity.



Scheme 1. Preparation of cap- and ZBG-bearing alkenes, validation and use in cross metathesis reaction.^a



a: i) K_2CO_3 , ACN, $Br-(CH_2)_3-CH=CH_2$. ii) Grubbs 1st generation catalyst, DCM, reflux, 6+1h. iii) CH_3OH , H_2SO_4 . iv) K_2CO_3 , DMF, $Br-(CH_2)_3-CH=CH_2$. v) 2nd generation catalyst, DCM, reflux. vi) H_2 , Pd/C, AcOEt. vii) TFA, DCM. viii) TFA:TES:DCM 1:0.1:1

Current compound design is focused on HDAC1-3, 4, 6 and 8 selective inhibitors due to a better biological knowledge. We previously validated cross metathesis (CM) to prepare alkyl-based hydroxamate and benzamide as HDACi.¹⁸ We present an extension with various ZBG: hydroxamic acids, thiols and benzamide as in SAHA, romidepsin and chidamide. Other ZBG were not explored.¹⁹ We selected indole and naphthyl²⁰ groups found as caps in HDACi. Indoles are known to be reluctant in CM reaction but their presence reduce HDACi cardiac toxicity.²¹ A naphthoxy group instead of a naphthylamide may comply with better plasma stability. Despite its simplicity our naphthyl series was unknown but similar to a “para” compound used to develop HDAC8 inhibitors with large cap groups.²²

The alkene **8** was prepared from thiol **7** (Scheme 1) to complement our library ZBG-protected alkenes **5** and **6**. A general TFA deprotection of the BOC and trityl groups was expected, with TES for the trityl one. The cap-bearing alkene **12** was prepared from naphthol **10**. The CM reactivity of alkenes **8** and **12** was verified and gave compounds **9** and **13** respectively in moderate to good yields. The CM between the ester **12** and the alkenes **5**, **6** and **8** gave access respectively to three alkenes **14-16** in good isolated yields with our continuous injection protocol of Grubbs 1st generation catalyst. The Grubbs 2nd generation catalyst was used for the benzamide **15**. The possible dimers formed in each case were separated. Compounds **14-16** were reduced to compounds **17**, **19** and **21** respectively, and deprotection gave the hydroxamate **18**, benzamide **20** and the thiol **22**. The direct CM with free NH indole remains difficult (Scheme S1, supporting information) and was partly solved by the methylation of the amide **23** to give **24**, still poor substrate for CM, even with the Grubbs 2nd generation catalyst, whatever the alkene used. In this series only the reduction of compound **27** to **29** worked and the deprotection of **29** did not allow recovery of the expected benzamide. The conversion of compound **24** to a butenylcarboline may be evaluated in the future in CM. These difficulties with the indole series prompted us to focus on the naphthyl series for biological testing. As a summary, Grubbs I catalyst is well suited for thioalkenes and N,O diBOC hydroxamates. The Grubbs II catalyst must be preferred for the benzamide derivatives, or other more reactive catalysts. The cap group should be apolar (supporting information, table S1).

Compounds **18**, **20** and **22** were tested for global HDAC inhibition using our BRET assays in living cells (Figure S1A-C, BRET principle, supplementary material).²³ SAHA ($EC_{50} = 1.68\mu M$) and CI-994 ($EC_{50} = 3.81\mu M$) were used as controls (Table 1, Figure S2A supplementary material) and gave results similar to previous studies.^{23,24} Compounds **18** and **20** were able to enter cells and to induce an increase of histone H3 acetylation, illustrated by an increase of the BRET signal. The absence of activity for thiol **22** may be due to the formation of a disulphide bridge as in psammaplins in the cellular environment. These experiments gave for the hydroxamate **18** an EC_{50} of $7.84\mu M$ and for the benzamides **20** an EC_{50} of $8.14\mu M$. Comparison of HDACi-induced BRET max values, obtained from dose-response experiments (Figure S2B, supplementary material) showed that compound **18**, SAHA and CI-994 lead to similar maximal level of histone H3 acetylation whereas compound **20** appeared significantly less active. The best HDACi **18** was further studied with SAHA and CI-994 as controls in a dose escalation experiments (Figure S3 supplementary material) for the simultaneous determination of viability (Table 2) and toxicity towards the selected cancer cells. These experiments demonstrated that all tested compounds decreased cancer cell viability through induction of toxicity (Figure S3 supplementary material). The IC_{50} obtained for the various cancer cell lines used (Table 2) is coherent with the EC_{50} obtained using BRET assay (Table 1). Compound **18** is less toxic than SAHA (about 4 fold) and A549 cells are the less sensitive to this compound. We noticed a correlation between induction of histone H3 acetylation and toxicity. For compound **18**, we determined HDAC and sirtuin selectively, using a standardized *in vitro* assay (Table 3, Figure S4 supplementary material). At $10\mu M$ concentration compound **18** was able to partially inhibit HDAC classes I (HDAC1,2,3,8), IIb (HDAC6,10) and IV (HDAC11), and no inhibition was noticed for class IIa and class III. 100% inhibition was obtained only for HDAC6 (class IIb). The dose-responses *in vitro* (Figure S4, supplementary material) showed that compound **18** is selective for HDAC6 ($IC_{50} = 95\text{ nM}$, Table 3), about tenfold less active for HDAC3, and 17 to 37-fold less for the other isoforms. The reference compound TSA was not selective, with better activity against HDAC HDAC1-3,6 and 10 than for other isoforms. The selective inhibition of HDAC6 prompted us to

examine histone H3 and α -tubulin acetylation in malignant pleural mesothelioma (MPM, meso 163) and lung adenocarcinoma (ADCA, A549) cells by western-blot. SAHA was used as a control for the induction of histone H3 and α -tubulin acetylation and CI-994 for the only induction of histone H3 acetylation. In meso 163 cells (Figure 2A upper panels), SAHA and compound **18** induced a rapid and transitory histone H3 acetylation whereas the benzamide CI-994 induced rapid

Table 1. EC₅₀ for the induction of histone acetylation measured by BRET assay in Met-5A pleural mesothelial cells.

Cpd.	18	20	SAHA	CI-994
EC ₅₀ (μ M)	7.84 \pm 0.18	8.14 \pm 0.32	1.68 \pm 0.19	3.81 \pm 0.17

EC₅₀ values were determined using GraphPad Prism, Prism 6 for Windows, by curve fitting using a sigmoidal dose-response model. Values represent means \pm standard error of at least three independent experiments.

Table 2. IC₅₀ (μ M) values for viability of Meso 163 and 13, A549 and ADCA72 cell lines treated with **18**, SAHA and CI-994 (72h).

Cpd.	Meso 13	Meso 163	A549	ADCA 72
SAHA	3.79 \pm 0.18	3.67 \pm 0.17	4.12 \pm 0.18	3.95 \pm 0.23
CI-994	7.83 \pm 0.19	15.77 \pm 0.19	15.96 \pm 0.19	3.90 \pm 0.18
18	15.62 \pm 0.12	15.86 \pm 0.14	62.36 \pm 0.18	15.72 \pm 0.16

IC₅₀ values were determined using GraphPad Prism, Prism 6 for Windows, by curve fitting using a sigmoidal dose-response model. Values represent means \pm standard error of at least three independent experiments.

Figure 2. Effect of compound **18** (20 μ M), SAHA (2.5 μ M) and CI-994 (10 μ M) on A) histone H3 and α -tubulin acetylation in MPM and lung ADCA cells. Meso 163 and A549 cells were treated with the compounds for 6 or 20h. Histone H3 and α -tubulin acetylation were analysed using western-blot. Left column indicates the molecular weight; and on B) E-cadherin, Sema-3F and P21 expression in MPM and lung ADCA cells. Meso 163 and A549 cells were treated with the compounds for 24h. mRNA expression of E-cadherin, Sema-3F and p21 was measured using real-time PCR. Results are means \pm S.E.M. of four independent experiments. * $p < 0.05$; ** $p < 0.01$; *** $p < 0.001$.

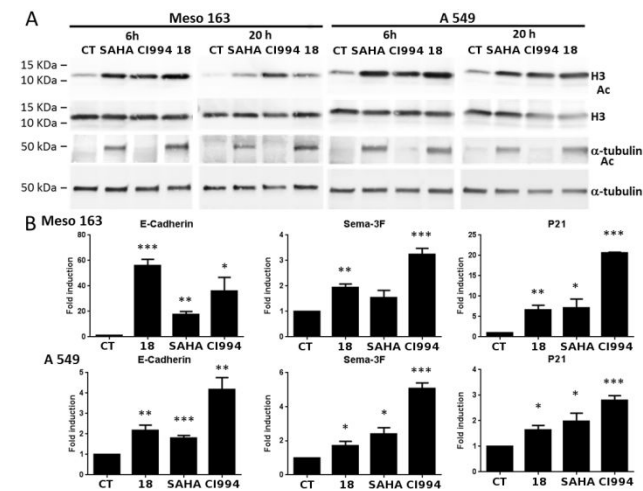


Figure 3. Comparative presentation of hydrophobic rim of the

and sustained histone H3 acetylation. The changes in histone H3 acetylation modulate the expression of a wide range of genes. In this study, we measured the mRNA level of E-cadherin, an 'epitheloid status' marker of epithelial to mesenchymal transition (EMT)²⁵ and the expression of two TSG was evaluated: Semaphorin-3F (Sema-3F) which reduces tumor angiogenesis and progression and which is lost or reduced in lung cancers,²⁶ and p21 involved in cell cycle.²⁷

Table 3. Inhibition profile and isoform selectivity of compound **18** compared to reference compounds.

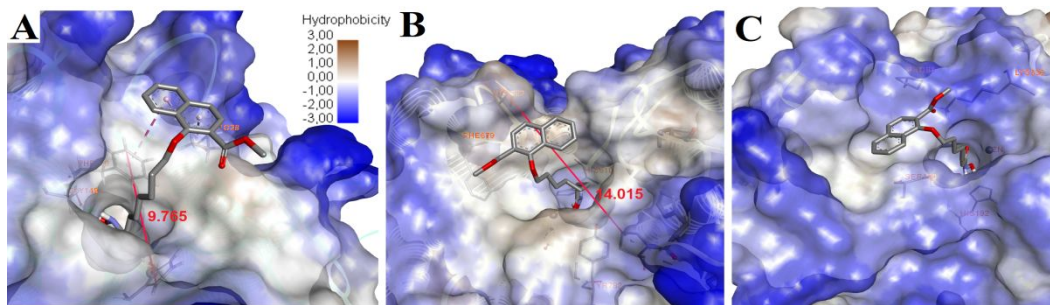
Target	% inhibition 18 , 10 μ M	Ref.	IC ₅₀ (μ M)	
			18	Ref.
HDAC1	84,7	TSA	3.5	0.011
HDAC2	67,1	TSA	3.4	0.016
HDAC3	87,9	TSA	1.0	0.010
HDAC4	-4,8	TSA	na	2.5
HDAC5	2,8	TSA	na	1.6
HDAC6	104,1	TSA	0.095	0.022
HDAC7	-16,3	TSA	na	0.98
HDAC8	93,1	TSA	1.6	0.79
HDAC9	-14,3	TSA	na	5.1
HDAC10	82,3	TSA	1.6	0.040
HDAC11	57,2	B	6.6	5.2
sirtuin1	-2,6	c	Nd	6.7
sirtuin2	-11,8	c	Nd	17
sirtuin3	-8,2	d	Nd	36
sirtuin6	-13,4	EX527		

TSA: (S)-trichostatin A. b: scriptaid. c: suramin. d: niacinamide. na: not active. Nd: not determined. Ref = reference compound.

Figure 2B shows that compound **18**, SAHA and CI-994 induced the expression of E-cadherin and of both TSGs suggesting a beneficial effect on MPM and lung cancer cells. Like SAHA, compound **18** induced a sustained α -tubulin acetylation demonstrating its inhibitory effect on cytoplasmic HDAC6, coherent with its high HDAC6 inhibition activity.²⁸ As expected, CI-994 did not increase α -tubulin acetylation according to the specific activity of benzamide on nuclear HDAC.²⁹ In A549 cells (Figure 2A lower panels), similar results were obtained. The only difference with meso 163 cells was the sustained activity of SAHA and compound **18** on histone H3 acetylation over time.

Insight into the ligand positioning and binding modes of compound **18** into eleven metal-dependant HDAC isoforms was performed by molecular docking study. Docking simulations were able to reproduce the co-crystal inhibitor binding modes with RMSD values below 1.5 Å for each isoform and took into account the important interactions between hydroxamic acid derivatives in the active center of HDAC isoforms.^{30,31} The method was additionally validated by comparing the ChemScore Fitness Function (CSFF) calculated for (S)-TSA and compound **18** with their experimentally obtained IC₅₀ values within the each isoform.³²

catalytic sites in HDAC1 homology model (A), crystal structure of human HDAC6 second catalytic domain (B), and first catalytic domain (C) with compound **18**.



GOLD CSFF values calculated for ligand-specific HDAC were in good agreement with the experimental inhibitory profile of (S)-TSA and compound **18** compared within the same isoform (Figures s5-s8 and Table s2, supplementary material). The compound **18** chelates with the Zn^{2+} ion inside the HDAC binding pockets, except for the isoforms which belong to the HDAC class IIa (HDAC5/HDAC7 and HDAC9). The binding modes of compound **18** into active pockets of HDAC1 and both catalytic domains of HDA6 are presented in Figure 3 (other HDACs in Figures s9-s20 and Table s2, supplementary material). HDAC6 CDII has a wider hydrophobic rim of the catalytic site (14.015 Å) comparing to the hydrophobic rim of HDAC1 (9.765 Å). Furthermore, the second argument for more favourable interaction of compound **18** with HDAC6 is a deeper active channel, which is less restricted for inhibitor access.³² The naphthalene moiety of compound **18** forms favourable π - π interaction with aromatic residue of Phe680 in HDAC6 CDII. In addition, π -Sulphur interactions are formed between Met682 and naphthalene ring (Figure S14, supplementary material). A bidentate binding mode was inspected for compound **18** inside the binding pocket of HDAC6, whereas the monodentate coordination was observed for the same compound in the active site of HDAC1. The high HDAC6 inhibitory potency of this compound could be explained by favourable interactions of the naphthalene CAP group with the side chains located in the outer rim of HDAC6 enzyme, as well as bidentate coordination with Zn^{2+} ion. Additionally, the higher HDAC6 potency of compound **18** may be also explained by the differences in the length of the active pockets. It is previously shown that the compounds with six carbon-spacer possess optimal distance between hydroxamic acid and CAP group for HDAC1 inhibitory activity.³³ When the spacer of the HDAC1 inhibitor is longer than six carbons, it is less favourable to make the hydrophobic interactions to the solvent exposed entrance of the catalytic site. Compound **18** has aliphatic linker constructed of eight carbon atoms, which may explain its selective HDAC6 inhibitory profile and less pronounced interactions with the side chains in the outer rim of class I HDACs. Domain-selective HDAC6 inhibitors studies³⁰ prompted us to examine possible domain selective affinity for compound **18**. We observed slightly different CSFF values calculated for (S)-TSA and compound **18** between HDAC6 catalytic domains (higher CSFF for CDI). To define whether the compound **18** possesses higher affinity for CDI of HDAC6 isoform, advanced structure based *in silico* and crystallographic studies should be performed, for the more precise determination of the ligand's domain selectivity.

In conclusion CM was successfully used to prepare rapidly with a generic method a series of alkyl-based HDAC inhibitors bearing the most common ZBGs and one of them is *in vitro* a nanomolar selective HDAC6 inhibitor. The method can be adapted to inhibitors of other relevant biological targets. The

methodology should be applicable in combinatorial strategies. Molecular docking rationalized the inhibition profile of compound **18**, introducing for the first time analysis of both CD1 and CD2 domains of HDAC6. The biological interest of compound **18** was demonstrated, with an increased acetylation of histones and α -tubulin, associated with the stimulation of the expression of E-cadherin, and TSGs such as SEMA3F and p21.

Experimental section

All biologically tested compounds were 95%+ pure as determined by HPLC. Typical synthetic sequence illustrated for compound **18**. DCM, dichloromethane; TFA, trifluoroacetic acid; TES: triethylsilane; EA, ethyl acetate; PE, petroleum ether; TEA, trimethylamine; ACN: acetonitrile.

Methyl (Z/E)-1-((8-((tert-butoxycarbonyl)((tert-butoxycarbonyl)oxy)amino)-8-oxooct-4-en-1-yl)oxy)-2-naphthoate **14.** Grubbs catalyst (50 mg) in DCM (3mL) was added over 6h (0,5mL/h rate) to a boiling solution of **5** (89mg, 0,33mmol) and **12** (208mg, 0,66mmol) in DCM (3mL) and refluxed 1h more. After cooling the solvent was removed (vacuum) and purification (flash chromatography silica, PE/EA/TEA 99.5/0/0.5, 250mL, 97/2.5/0.5, 1L, 94.5/5/0.5, 1L followed by preparative thin layer chromatography PE/EA: 97.5/2.5 and 95/5) gave **14** (88mg, 48%) as an orange oil. ¹H NMR (CDCl₃) δ ppm: 1.53 (4s, 18H), 2.02 (m, 2H), 2.34 (m, 4H), 2.92 (m, 2H), 3.95 (3s, 3H), 4.12 (dt, 2H, J=1.0, 6.6 Hz), 5.55 (m, 2H), 7.58 (m, 3H), 7.84 (m, 2H), 8.27 (dd, 1H, J=6.49, 7.33Hz). ¹³C NMR (CDCl₃) δ ppm: 23.9, 27.4, 27.5, 27.9, 28.0, 29.05, 29.1, 30.1, 30.3, 30.4, 36.8, 52.2, 85.2, 86.0, 119.2, 123.4, 123.7, 126.4, 126.7, 127.8, 128.3, 128.8, 129.7, 130.2, 130.8, 136.7, 157.4, 166.9, 170.2. HRMS Calcd. for C₃₀H₃₉NNaO₉ [M+Na]⁺: 580,2517, Found: 580.2524.

Methyl 1-((8-(hydroxyamino)-8-oxooctyl)oxy)-2-naphthoate **18.** TFA (0.33mL, 4mmol) was added to a solution of **17** (84mg, 0.15mmol) in DCM and the solution stirred for 3h. The crude mixture was diluted with EA and washed (saturated aqueous NaCl 3x5mL). The combined aqueous extracts were neutralized (saturated aqueous NaHCO₃, pH7) and extracted (EA, 3x20mL). The combined organic layers were dried (MgSO₄) and concentrated under vacuum to yield **18** (20mg, 36%) as an orange oil. ¹H NMR (CDCl₃) δ ppm: 1.33 (m, 4H), 1.52 (m, 4H), 1.85 (t, 2H, J=7.4Hz), 1.96 (t, 2H, J=7.3Hz), 3.89 (s, 3H), 4.05 (t, 2H, J=6.5Hz), 7.66 (m, 2H), 7.75 (s, 2H), 7.99 (dd, 1H, J=6.1, 7.1Hz), 8.19 (dd, 1H, J=6.3, 7.2Hz), 8.69 (s, 1H), 10.37(s, 1H). ¹³C NMR (CDCl₃) δ ppm: 25.6, 25.9, 29.0, 29.1, 30.2, 32.7, 52.7, 76.4, 119.8, 123.5, 123.9, 126.7, 127.4, 128.5, 128.5, 129.0, 136.5, 156.6, 166.8, 169.6. HRMS Calcd. for C₂₀H₂₅NNaO₅ [M+Na]⁺: 382.1625, Found: 382.1626.

ASSOCIATED CONTENT

Supporting Information. Synthesis, characterizations for all compounds, ¹H/¹³C NMR spectra and HPLC data for compounds **18**, **20** and **22**, biological experiments, docking methods, Figures

S1-S20. Authors will release the PDB files upon article publication. The Supporting Information is available free of charge on the ACS Publications website.

AUTHOR INFORMATION

Corresponding Author. *Dr. Philippe BERTRAND, Philippe.bertrand@univ-poitiers.fr.

Author Contributions. The manuscript was written through contributions of all authors.

Funding Sources. Regions Nouvelle Aquitaine and Pays de la Loire, Ligue Contre le Cancer: committees of Vendée and Charente-Maritime, D.A., K.N., and D.R. acknowledge the project (contract no. 172033) supported by the Ministry of Education, Science, and Technological Development of the Republic of Serbia.

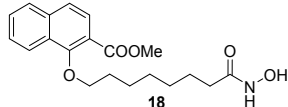
ACKNOWLEDGMENT

Authors thank the Centre National de la Recherche Scientifique, University of Poitiers, COST Action CM1406, Professor Olaf Wiest group for providing us homology models of eleven HDAC isoforms (HDAC1-HDAC11) used for molecular docking study.

REFERENCES

- Duvic, M.; Vu, J. Vorinostat: A New Oral Histone Deacetylase Inhibitor Approved for Cutaneous T-Cell Lymphoma. *Expert Opin. Investig. Drugs* **2007**, *16*, 1111–1120.
- Poole, R. Belinostat: First Global Approval. *Drugs* **2014**, *74*, 1543–1554.
- Fenichel, M. P. FDA Approves New Agent for Multiple Myeloma. *J. Natl. Cancer Inst.* **2015**, *107*, djv165.
- Grant, C.; Rahman, F.; Piekarz, R.; Peer, C.; Frye, R.; Robey, R. W.; Gardner, E. R.; Figg, W. D.; Bates, S. E. Romidepsin: A New Therapy for Cutaneous T-Cell Lymphoma and a Potential Therapy for Solid Tumors. *Expert Rev. Anticancer Ther.* **2010**, *10*, 997–1008.
- Shi, Y.; Jia, B.; Xu, W.; Li, W.; Liu, T.; Liu, P.; Zhao, W.; Zhang, H.; Sun, X.; Yang, H.; Zhang, X.; Jin, J.; Jin, Z.; Li, Z.; Qiu, L.; Dong, M.; Huang, X.; Luo, Y.; Wang, X.; Wang, X.; Wu, J.; Xu, J.; Yi, P.; Zhou, J.; He, H.; Liu, L.; Shen, J.; Tang, X.; Wang, J.; Yang, J.; Zeng, Q.; Zhang, Z.; Cai, Z.; Chen, X.; Ding, K.; Hou, M.; Huang, H.; Li, X.; Liang, R.; Liu, Q.; Song, Y.; Su, H.; Gao, Y.; Liu, L.; Luo, J.; Su, L.; Sun, Z.; Tan, H.; Wang, H.; Wang, J.; Wang, S.; Zhang, H.; Zhang, X.; Zhou, D.; Bai, O.; Wu, G.; Zhang, L.; Zhang, Y. Chidamide in Relapsed or Refractory Peripheral T Cell Lymphoma: A Multicenter Real-World Study in China. *J. Hematol. Oncol. J Hematol Oncol* **2017**, *10*, 69.
- Azad, N.; Zahnow, C. A.; Rudin, C. M.; Baylin, S. B. The Future of Epigenetic Therapy in Solid Tumours: Lessons from the Past. *Nat Rev Clin Oncol* **2013**, *10*, 256–266.
- Arrowsmith, C. H.; Bountra, C.; Fish, P. V.; Lee, K.; Schapira, M. Epigenetic Protein Families: A New Frontier for Drug Discovery. *Nat Rev Drug Discov* **2012**, *11*, 384–400.
- Feng, D.; Wu, J.; Tian, Y.; Zhou, H.; Zhou, Y.; Hu, W.; Zhao, W.; Wei, H.; Ling, B.; Ma, C. Targeting of Histone Deacetylases to Reactivate Tumour Suppressor Genes and Its Therapeutic Potential in a Human Cervical Cancer Xenograft Model. *PLoS ONE* **2013**, *8*, e80657.
- Wagner, T.; Brand, P.; Heinzel, T.; Krämer, O. H. Histone Deacetylase 2 Controls P53 and Is a Critical Factor in Tumorigenesis. *Biochim. Biophys. Acta BBA - Rev. Cancer* **2014**, *1846*, 524–538.
- Ma, Y.; Jin, H.; Wang, X.; Shin, V. Y.; Chen, D.; Chen, Y.; Feng, L.; Xu, W.; Lin, X.; Chu, J.; Sun, J.; Pan, M.; Yue, Y. Histone Deacetylase 3 Inhibits New Tumor Suppressor Gene DTWD1 in Gastric Cancer. *Am J Cancer Res* **2015**, *5*, 663–673.
- Mottamal, M.; Zheng, S.; Huang, L. T.; Wang, G. Histone Deacetylase Inhibitors in Clinical Studies as Templates for New Anticancer Agents. *Molecules* **2015**, *20*.
- Roche, J.; Bertrand, P. Inside HDACs with More Selective HDAC Inhibitors. *Eur. J. Med. Chem.* **2016**, *121*, 451–483.
- Robey, R. W.; Chakraborty, A. R.; Basseville, A.; Luchenko, V.; Bahr, J.; Zhan, Z.; Bates, S. E. Histone Deacetylase Inhibitors: Emerging Mechanisms of Resistance. *Mol. Pharm.* **2011**, *8*, 2021–2031.
- Hermant, P.; Bosc, D.; Piveteau, C.; Gealageas, R.; Lam, B.; Ronco, C.; Roignant, M.; Tolojanahary, H.; Jean, L.; Renard, P.-Y.; Lemdani, M.; Bourotte, M.; Herledan, A.; Bedart, C.; Biela, A.; Leroux, F.; Deprez, B.; Deprez-Poulain, R. Controlling Plasma Stability of Hydroxamic Acids: A MedChem Toolbox. *J. Med. Chem.* **2017**, *60*, 9067–9089.
- Witt, O.; Deubzer, H. E.; Milde, T.; Oehme, I. HDAC Family: What Are the Cancer Relevant Targets? *Cancer Lett.* **2009**, *277*, 8–21.
- Bressi, J. C.; Jennings, A. J.; Skene, R.; Wu, Y.; Melkus, R.; Jong, R. D.; O'Connell, S.; Grimshaw, C. E.; Navre, M.; Gangloff, A. R. Exploration of the HDAC2 Foot Pocket: Synthesis and {SAR} of Substituted N-(2-Aminophenyl)Benzamides. *Bioorg. Med. Chem. Lett.* **2010**, *20*, 3142–3145.
- Estiu, G.; Greenberg, E.; Harrison, C. B.; Kwiatkowski, N. P.; Mazitschek, R.; Bradner, J. E.; Wiest, O. Structural Origin of Selectivity in Class II-Selective Histone Deacetylase Inhibitors. *J. Med. Chem.* **2008**, *51*, 2898–2906.
- Zwick, V.; Nurisso, A.; Simões-Pires, C.; Bouchet, S.; Martinet, N.; Lehotzky, A.; Ovadi, J.; Cuendet, M.; Blanquart, C.; Bertrand, P. Cross Metathesis with Hydroxamate and Benzamide BOC-Protected Alkenes to Access {HDAC} Inhibitors and Their Biological Evaluation Highlighted Intrinsic Activity of BOC-Protected Dihydroxamates. *Bioorg. Med. Chem. Lett.* **2016**, *26*, 154–159.
- Bertrand, P. Inside HDAC with HDAC Inhibitors. *Eur. J. Med. Chem.* **2010**, *45*, 2095–2116.
- Valente, S.; Trisciuglio, D.; De Luca, T.; Nebbioso, A.; Labella, D.; Lenoci, A.; Bigogno, C.; Dondio, G.; Miceli, M.; Brosch, G.; Del Bufalo, D.; Altucci, L.; Mai, A. 1,3,4-Oxadiazole-Containing Histone Deacetylase Inhibitors: Anticancer Activities in Cancer Cells. *J. Med. Chem.* **2014**, *57*, 6259–6265.
- Shultz, M. D.; Cao, X.; Chen, C. H.; Cho, Y. S.; Davis, N. R.; Eckman, J.; Fan, J.; Fekete, A.; Firestone, B.; Flynn, J.; Green, J.; Growney, J. D.; Holmqvist, M.; Hsu, M.; Jansson, D.; Jiang, L.; Kwon, P.; Liu, G.; Lombardo, F.; Lu, Q.; Majumdar, D.; Meta, C.; Perez, L.; Pu, M.; Ramsey, T.; Remiszewski, S.; Skolnik, S.; Traebert, M.; Urban, L.; Uttamsingh, V.; Wang, P.; Whitebread, S.; Whitehead, L.; Yan-Neale, Y.; Yao, Y.-M.; Zhou, L.; Atadja, P. Optimization of the in Vitro Cardiac Safety of Hydroxamate-Based Histone Deacetylase Inhibitors. *J. Med. Chem.* **2011**, *54*, 4752–4772.
- Tang, W.; Luo, T.; Greenberg, E. F.; Bradner, J. E.; Schreiber, S. L. Discovery of Histone Deacetylase 8 Selective Inhibitors. *Recent Adv. Med. Chem.* **2011**, *21*, 2601–2605.
- Blanquart, C.; François, M.; Charrier, C.; Bertrand, P.; Grégoire, M. Pharmacological Characterization of Histone Deacetylase Inhibitor and Tumor Cell-Growth Inhibition Properties of New Benzofuranone Compounds. *Curr. Cancer Drug Targets* **2011**, *11*, 919–928.
- Delatouche, R.; Denis, I.; Grinda, M.; El Bahhaj, F.; Baucher, E.; Collette, F.; Heroguez, V.; Gregoire, M.; Blanquart, C.; Bertrand, P. Design of PH Responsive Clickable Prodrugs Applied to Histone Deacetylase Inhibitors: A New Strategy for Anticancer Therapy. *Eur J Pharm Biopharm* **2013**, *85*, 862–72.
- Ohira, T.; Gemmill, R. M.; Ferguson, K.; Kusy, S.; Roche, J.; Brambilla, E.; Zeng, C.; Baron, A.; Bemis, L.; Erickson, P.; Wilder, E.; Rustgi, A.; Kitajewski, J.; Gabrielson, E.; Bremnes, R.; Franklin, W.; Drabkin, H. A. WNT7a Induces E-Cadherin in Lung Cancer Cells. *Proc. Natl. Acad. Sci.* **2003**, *100*, 10429–10434.
- Potiron, V. A.; Roche, J.; Drabkin, H. A. Semaphorins and Their Receptors in Lung Cancer. *Cancer Lett.* **2009**, *273*, 1–14.
- Abbas, T.; Dutta, A. P21 in Cancer: Intricate Networks and Multiple Activities. *Nat Rev Cancer* **2009**, *9*, 400–414.
- Hubbert, C.; Guardiola, A.; Shao, R.; Kawaguchi, Y.; Ito, A.; Nixon, A.; Yoshida, M.; Wang, X.-F.; Yao, T.-P. HDAC6 Is a Microtubule-Associated Deacetylase. *Nature* **2002**, *417*, 455–458.
- Bracker, T. U.; Sommer, A.; Fichtner, I.; Faus, H.; Haendler, B.; Hess-Stumpff, H. Efficacy of MS-275, a Selective Inhibitor of Class I Histone Deacetylases, in Human Colon Cancer Models. *Int. J. Oncol.* **2009**, *35*, 909–920.

- 1
2
3
4
5
6
7
8
9
10
11
12
13
14
15
16
17
18
19
20
21
22
23
24
25
26
27
28
29
30
31
32
33
34
35
36
37
38
39
40
41
42
43
44
45
46
47
48
49
50
51
52
53
54
55
56
57
58
59
60
30. Hai, Y.; Christianson, D. W. Histone Deacetylase 6 Structure and Molecular Basis of Catalysis and Inhibition. *Nat Chem Biol* **2016**, *12*, 741–747.
31. Zhou, J.; Li, M.; Chen, N.; Wang, S.; Luo, H.-B.; Zhang, Y.; Wu, R. Computational Design of a Time-Dependent Histone Deacetylase 2 Selective Inhibitor. *ACS Chem. Biol.* **2015**, *10*, 687–692.
32. Miyake, Y.; Keusch, J. J.; Wang, L.; Saito, M.; Hess, D.; Wang, X.; Melancon, B. J.; Helquist, P.; Gut, H.; Matthias, P. Structural Insights



in vitro
HDAC6: 95 nM
HDAC1-3,8: 1-3.5 μ M
HDAC10: 1.6 μ M
HDAC11: 6.6 μ M
HDAC4-7,9: not active



- into HDAC6 Tubulin Deacetylation and Its Selective Inhibition. *Nat Chem Biol* **2016**, *12*, 748–754.
33. Schäfer, S.; Saunders, L.; Eliseeva, E.; Velena, A.; Jung, M.; Schwienhorst, A.; Strasser, A.; Dickmanns, A.; Ficner, R.; Schlimme, S.; Sippl, W.; Verdin, E.; Jung, M. Phenylalanine-Containing Hydroxamic Acids as Selective Inhibitors of Class IIb Histone Deacetylases (HDACs). *Bioorg. Med. Chem.* **2008**, *16*, 2011–2033.